PAPILLOMAVIRUS L2-DEPENDENT ENDOCYTOSIS AND SUBCELLULAR TRAFFICKING

by

Mingfeng Lu

A Thesis Submitted to the Faculty of the

Department of Cellular and Molecular Medicine

In Partial Fulfillment of the Requirements

For the Degree of

Master of Science

In the Graduate College

THE UNIVERSITY OF ARIZONA

2016

STATEMENT BY AUTHOR

The thesis titled *Papillomavirus L2-dependent endocytosis and subcellular trafficking* prepared by *Mingfeng Lu* has been submitted in partial fulfillment of requirements for a master's degree at the University of Arizona and is deposited in the University Library to be made available to borrowers under rules of the Library.

Brief quotations from this thesis are allowable without special permission, provided that an accurate acknowledgement of the source is made. Requests for permission for extended quotation from or reproduction of this manuscript in whole or in part may be granted by the copyright holder.

SIGNED: *Mingfeng Lu*

APPROVAL BY THESIS DIRECTOR

This thesis has been approved on the date shown below:

Samuel K Campos
Assistant Professor of Immunology

07/15/2016
Date

Table of Contents

Abstract

Human papillomaviruses (HPV) are among the most common sexually transmitted infections and are responsible for 5% of all human cancers. HPV type 16 is the most prevalent of the high-risk HPVs (a subgroup of HPVs with potential to cause cancer), accounting for ~55% of HPV-associated cancers. HPV16 is a nonenveloped virus, composed of the major capsid protein L1, the minor capsid protein L2, and a circular double-stranded DNA genome (vDNA) condensed with human histones. HPV initially infects undifferentiated basal keratinocytes and viral replication is dependent on epithelial differentiation. Like many other DNA viruses, HPV must deliver its vDNA to the host cell nucleus to successfully replicate. Initial binding of HPV16 to host cells is through L1 interactions with cell surface heparan sulfate receptors. Shortly after virus binding, L2 is believed to undergo furin cleavage-dependent conformational changes, resulting in spanning of the protein across the local membrane and exposure of the central and C-terminal regions of L2 (which was lumenal and and inaccessible before furin cleavage) to the host cell cytosol. L2 is critical for transport of the L2/vDNA from endosomes to the trans-Golgi network (TGN). We hypothesize that furin-dependent early L2 spanning, through the direct binding and recruitment of cytosolic sorting factors, may contribute to viral endocytosis and subcellular retrograde trafficking (trafficking from endosomes to Golgi) of vDNA. We have developed a Tac receptor (CD25 or IL2 receptor, a transmembrane cell surface protein) chimera system to study L2-dependent endocytosis and trafficking. In this system the Tac ecto- and transmembrane domains are fused to the ~400 amino acid portion of L2 that is likely

cytosolic upon L2 spanning. Through transient expression of Tac-L2 chimera we use anti-Tac ectodomain antibodies to label and track cell surface populations by immunofluorescence and confocal microscopy. We have also adopted this system to study endocytosis through a cell surface biotinylation approach. Both approaches suggest that L2 may enhance endocytosis and preliminary evidence suggests that the Tac-L2 chimera may recruit the cytosolic retromer complex (the host cytosolic factors help protein retrograde trafficking) to preferentially traffic to the TGN. Retromer-dependent trafficking of cargo from early endosomes to the TGN is known to involve certain members of the sorting nexin family, specifically the SNX-BAR proteins. We performed a small siRNA screen and identify SNX6 and SNX32 (aka SNX6b) as SNX-BAR proteins that may be specifically involved in retrograde trafficking of HPV16 L2/vDNA during infection. Future work will focus on the mechanisms through which L2 and SNX6 influence HPV16 entry and trafficking.

Introduction

The human papillomavirus family and its structure

Human papillomavirus (HPV) is a non-enveloped double-stranded circular DNA virus from the papillomaviridae family that is capable of infecting human keratinocytes [1]. Many different types of HPVs have been identified and are detected in epithelium of the oral mucosa, larynx, trachea, skin, anogenital tract, and urethra [2]. They can be divided into 2 broad groups based on their tropism: the cutaneous viruses that infect skin and the mucosal viruses that infect oral and anogenital mucosa [3]. They can also be divided into low-risk and high-risk groups based on the lesions they can induce [4]. Most low-risk HPV infections are transient and asymptomatic, and induce only benign warts that typically regress spontaneously due to host immune response. In normal populations without immunosuppression or genetic predispositions, low-risk HPVs are very rarely associated with neoplasia or cancer. Like low-risk HPVs, high-risk HPVs typically cause asymptomatic or benign lesions in most individuals. However, persistent high-risk HPV infections with deregulated viral gene expression can disturb the normal keratinocyte physiology, stimulating abnormal cell proliferation to promote immortalization and progression towards cancer [5]. Accordingly, persistent infections by high-risk HPVs are associated with cervical cancers, many other anogenital cancers, and a rising incidence of head/neck cancers [6,7].

The structure of HPV is relatively simple. The viral particle, or virion, is about 55 nm in diameter. The capsid consists of two proteins (Fig. 1A). The major capsid protein L1 is arranged as 72 pentamers, forming the basic structure of icosahedral capsid [1],

and is involved in initial cell surface binding [8]. L1 pentamers can also assemble themselves into empty capsid (virus-like particles) in the absence of any other proteins [9], and for a long time L1 was thought to be the key factor for virus infection and the importance of L2 was not appreciated. Recent evidence suggests that L2, the minor viral capsid protein, plays a critical role in the subcellular trafficking of the HPV genome during initial HPV infection. L2 is mostly buried underneath the L1 pentamers, except some residues at the N terminus are exposed on the viral capsid surface [10].

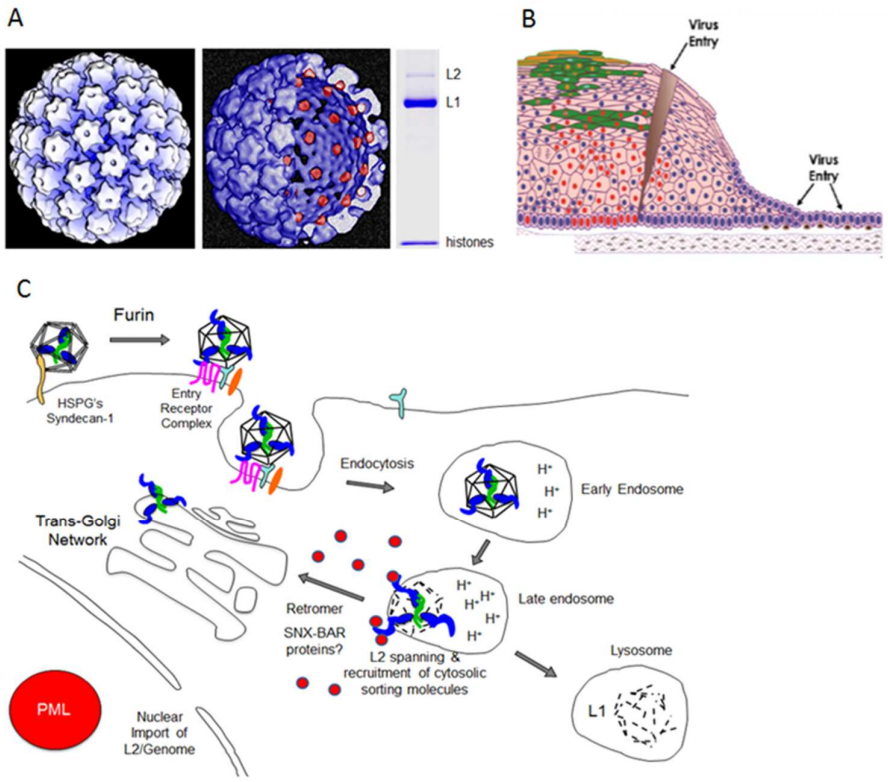

Fig 1. HPV structure and infection pathway. (A) HPV capsid is composed of two proteins: L1 is the major protein form 72 disulfide-linked pentamers, and L2 (red density), the minor protein buried underneath L1 and attached to the viral genome. (B) HPV can get access to and infect undifferentiated basal lamina keratinocytes when microwounds occur on the epidermis, replicates itself during keratinocyte life cycle as the cells move towards surface skin (modified from [5]). (C) HPV interacts with cell surface receptors, is then taken up through endocytosis and transported into early endosomes. During endosomal acidification the virus capsid disassembles. L1 is degraded in the lysosome, L2 together with the virus genome are directed to the TGN by interacting with host cell factors. During cell mitosis the L2/viral genome are somehow translocated into the cell nucleus.

L2 is complexed to the 8 kb circular viral dsDNA genome, which is condensed with histones [11]. A lot of evidence suggested L2 is not merely a structural protein but has many additional functions during infection. L2 facilitates virus escape from endosomal degradation and helps the genome traffic into the trans Golgi network (TGN) by interacting with sorting nexin 17 and the retromer complex [12, 48] (Fig 1C). It may also interact with dynein light chains to transport virus towards the host cell nucleus [13].

Infection and pathogenesis of human papillomavirus

Human skin epithelial tissue is composed of differentiating keratinocyte layers organized above the basement membrane. When an epithelial micro-wound occurs (Fig.1B), HPV can get access to the basement membrane to infect the undifferentiated basal keratinocytes [14]. This initial infection is followed by viral genome replication and maintenance of the viral genomic episome at low copy number [15]. During the initial infection viral proteins play different roles in replication. The E1 protein assembles as a hexamer on the viral origin of replication [16]. E2 is a DNA binding transcription factor that can also help recruit E1 to the viral origin during genome replication [5], and it also controls the expression of E6, E7, E1 and E2, itself [17]. E2 also regulates accurate genome partitioning during cell division by physically tethering the viral genome to mitotic chromosomes [18]. E6 and E7 have the ability to modulate the host cell-cycle, enabling otherwise differentiating cells to enter S phase allowing for viral genome replication [19].

Infected basal stem cells form a reservoir of infection as the viral episome is maintained at low copy number [5]. As basal cells divide and push upwards into the epidermis, virus genomes are replicated and carried by differentiating daughter cells [20]. Viral oncogenes have the ability to force cells into the cell cycle. The E6 oncoprotein can associate with host proteins and increase p53 (a tumor suppressor) proteosomal degradation to avoid host cell apoptosis [33]. E7 can bind and inactivate pRb (retinoblastoma), which is an important tumor suppressor that inhibits cell cycle progression [21]. The late viral promoter is activated in the upper spinous epithelial layers, and viral late proteins (including capsid proteins) are expressed at high levels [22]. The viral genome copy numbers also increase dramatically [23]. After genome amplification, virus capsid proteins L1 and L2 are expressed and progeny virions are assembled in granular layer cells. Finally viruses are shed into the environment with the dead desquamated cells. The replication of the virus in these cell layers contributes to their avoidance of the host immune responses [24].

HPV immune evasion and persistence

HPV has evolved a variety of mechanisms to avoid the host immune response. First, HPV is a non-lytic virus, and its infection causes no cell death. As mentioned above, it utilizes the natural death and disintegration of the upper epithelium, and the newly-replicated progeny virus is shed with dead keratinocytes from skin surface. This life cycle limits the opportunity of antigen presentation cells (APC) to digest and present viral antigen peptides to the host immune system [26]. Additionally, the viral proteins

expressed during infection also contribute to its avoidance of the immune response. E7 can down-regulate the host transporter associated with antigen processing protein 1 (TAP1), which transports antigen from the cytoplasm to the endoplasmic reticulum, thus decreasing antigen availability for binding to MHC class I (MHC-I) molecules [27]. E6 and E7 can down-regulate the transcription of TLR9, which is important in recognizing viral dsDNA and activating the innate immune responses [28]. E6 and E7 can also down-regulate expression of IFN-α and IFN-β, which has anti-viral and anti-tumor functions during virus infection [29].

HPV16 also seems to somehow reduce Langerhans cell (LC) numbers. LCs are resident dendritic cells in skin and mucosa, crucial to the initiation of adaptive immune response and LCs are very depleted in dysplastic cervical tissue [67,70]. HPV16 may achieve this by decreasing surface expression of E-cadherin on infected keratinocytes. E-cadherin is an important adhesion factor that mediates LCs retention on keratinocytes, and early viral proteins in lower-layer keratinocytes may reduce cell surface E-cadherin expression [69]. Additionally, interaction between HPV16 and LCs through the PI3-K/Akt signaling pathway may suppress LC activation [73]. Research also shows LCs exposed to HPV types 18, 31, 45, 11 and HPV5 lack costimulatory molecule (important signaling molecules during antigen presentation) expression, cytokine and chemokine secretion and migratory ability, and they have deregulated cellular signaling [74].

Despite viral immune evasion mechanisms, HPV infections can eventually cause activation of the adaptive immune response. Langerhans cells can engulf dead or dying

infected keratinocytes, allowing host APCs to get access to virus L1 capsid protein and oncoprotein E7 for antigen presentation [26,71]. After taking up infected cell debris, Langerhans cells become migratory, losing their endocytic and antigen processing potential, migrate to local lymph nodes, and present antigens to naive T cells [68]. Those naive T cells that encounter specific antigen will stop migrating and start proliferating and differentiating into effecter cells. The primed CD8+ T cells are then attracted by chemokines and traffic back into infected epithelial tissues. They can then kill those infected cells efficiently and usually viruses are eliminated and lesions will regress [25].

Accidental integration and consequences: cervical cancer and mechanism of oncogenesis

HPV infections are quite universal during the female life span. Although most HPV-induced lesions will regress spontaneously and few infected woman will get invasive disease [30], it is thought that persistent high-risk HPV infection is the greatest risk factor for anogenital malignancies, such as cervical cancer. It is reported that the viral genome can be found in more than 95% of cervical cancer biopsies [31]. Cervical cancer is the second most frequent cancer in women in the world. In 2012, about 445,000 new cervical cancer cases were identified and about 270,000 people died because of cervical cancer. In total, infections by high-risk HPVs are responsible for an astounding 5% of cancers worldwide [32].

So what is the linkage between persist high-risk virus infection and its malignancy mechanism? As mentioned before, the HPV life cycle is tightly linked to the epithelial cell differentiation, Initially it is necessary for the virus to maintain low copy number in the nuclei of undifferentiated host cells. This forms a reservoir because they are nonlytic and progeny viruses are shed in dead epithelial squamous cells. It is reasonable for the virus to possess mechanisms to induce growth-arrested differentiated epithelial cells to reenter the cell cycle for the purpose of viral genome synthesis, and the ability of high-risk HPV to establish persist infection directly contributes to its oncogenic potential [21]. Certain viral proteins seem to play important roles in oncogenesis. The E6 oncoprotein can associate with host E6AP, an E3 ubiquitin ligase, to increase p53 (a tumor suppressor) proteosomal degradation. This avoids cell apoptosis [33]. It is also found to upregulate telomerase activity, thus promoting cellular immortalization and transformation [34]. The E7 oncoprotein binds to retinoblastoma protein (pRB inhibits cell cycle progression) and inactivates it, thus increasing cell division [35]. During the stage of low-copy episome maintainance, the expression of the E6 and E7 oncogenes used for viral replication are tightly regulated by other viral proteins, so the infected cells will be lost with the dead squamous epithelium, and this process will lead to progeny virus but will cause no cancer [36]. However, in some cases the viral E6 and E7 oncogenes will integrate into cellular genome accidentally, whereas other genes which functions to repress these oncogenes are deleted or their expression is disturbed [37]. This may lead to deregulated high level expression of E6/E7, and the cells with integrated E6/E7 have a selective growth advantage compared with those cells have

only episomal HPV genomes [38]. This seems to play an important role in progression of cervical dysplasia, as HPV genomes are found to be integrated in many advanced preneoplastic cervical lesions and carcinomas [39]. However, the integration is really accidental for the viral life cycle because many viral genes needed for virion synthesis are deleted and it's a dead end for an infectious virus [36].

Virus binding, entry, and subcellular trafficking in infected basal keratinocytes

It is essential for HPV to deliver its viral genome into the host cell nucleus and the HPV capsid has evolved special structures to achieve this (Fig.1C). For HPV16, the L1 capsid protein initially binds to epithelial cell surface heparin sulfate proteoglycans (HSPGs), causing a conformational changes which increases accessibility of the L2 N-terminus [40]. This is thought to be facilitated by cyclophilin B (CyPB) [41]. After that, a highly conserved consensus furin convertase site (9-RTKR-12, L2 N-terminus) becomes accessible to furin and related proprotein convertases (PC) 5/6 [42]. L2 is then cleaved and the capsid is believed to transfer to an as yet unidentified cell-surface receptor to be endocytosed and begin its intracellular trafficking [43].

After HPV is internalized, the virus is trafficked into early endosomes and it is believed that endosomal acidification is important for virus capsid disassembly and egress from endosomes [43,44]. L1 dissociates from L2 and the viral genome, remaining in the late endosome and lysosomal compartments to be degraded [45]. However, the L2 protein has a transmembrane domain which somehow enables L2 to span through the endosomal membrane to interact with host cytosolic sorting factors

and direct its retrograde trafficking [46]. L2 spanning is believed to occur after a capsid conformational change due to furin cleavage [47]. Our unpublished data also shows that L2 fails to reach the Golgi when furin cleavage is blocked, suggesting that L2 spanning was triggered by furin cleavage very early on cell membrane before endocytosis.

The exposed cytosolic part of L2 has sequences able to interact with cytosolic sorting factors, and this is believed to contribute to virus escape from endosomes and transport into the trans-Golgi network (TGN) to avoid lysosomal degradation. There are many candidates for such interaction sequences and two of them seem to be most important. One is NPAY at residues 254-257, a highly conserved sorting nexin 17 (SNX17) binding motif. Research shows that SNX17 binding is essential for L2 retention in late endosomes, allowing the L2-genome complex to have enough time to egress by retromer-mediated trafficking and avoid rapid lysosomal degradation, or even directly help L2-genome complex egress together with retromer [12]. Another important motif is FYL and YYML at residues 446-448 and 452-455, located close to the C-terminus of L2. These motifs resemble known retromer binding motifs and interact with retromer complex directly to mediate retrograde trafficking [48], and we will mainly focus on the important role of retromer during virus infection.

Retromer and retrograde transport

The mammalian retromer is a multisubunit complex that mediates retrograde transport of transmembrane cargos from endosomes to the TGN. There are two main

components of retromer: sorting nexin (SNX) dimer and the vacuolar protein sorting (Vps) 26/29/35 trimer [49, 50] (Fig.2A).

Sorting nexins are a family of proteins localized in the cytoplasm which has the ability for membrane association through its phox-homology (PX) domain [51]. Currently there are 33 known sorting nexins. Different sorting nexins play diverse roles in cells, such as endosomal recycling, endosomal sorting, endosomal signaling and endocytosis [50] (Fig.2D). There is a subfamily of sorting nexins called SNX–BARs because of one BAR (Bin/Amphiphysin/Rvs) domain in addition to the PX domain. There are a total of12 SNX-BAR proteins (SNX1, SNX2, SNX4, SNX5, SNX6, SNX7, SNX8, SNX9, SNX18, SNX32 and SNX33) [52]. They attract more interest in our research due to their BAR domain properties. The BAR domain can help SNX form a rigid curved dimer (Fig.2B). Its concave face can recognize and interact with positive membrane curvature. Some evidence shows SNX–BARs can also induce membrane tubulations (the important endosomal sorting platforms) [53] (Fig.2C). The PX domain can bind to phosphatidylinositol-3-monophosphate (PtdIns3P), which is enriched in the early endocytic network [54]. Both the PX domains and BAR domains are required for SNX–BARs to associate with membranes [52]. In some SNX-BARs there is an additional amphipathic helix (AH) structure at the N-terminus which can detect membrane curvature located in BAR domain, and this can help SNX-BAR be recruited to curved membranes [55].

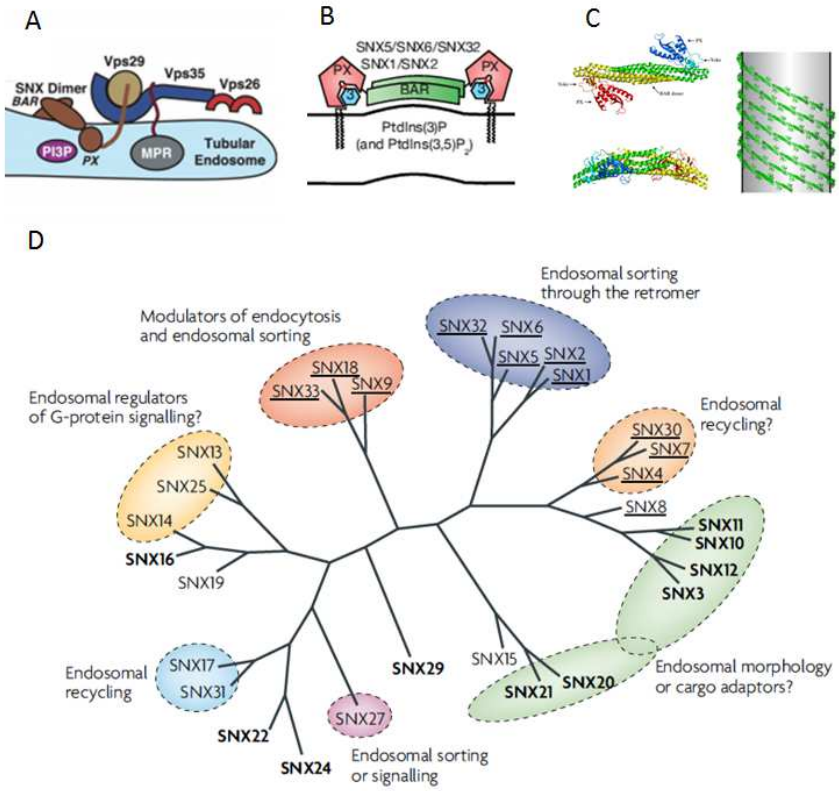

Fig 2. Retromer and SNX structure. (A) Retromer consists of the Vps26, Vps29 and Vps35 trimer and the SNX-BAR dimer. Vps trimer plays an important role in transmembrane cargo selection (from [59]). (B)SNX-BAR dimer can bind and induce endosomal membrane tabulation (from [53]). (C) SNX can form homodimers or heterodimers through its BAR domains and form the curvature structure, which plays an important role in endosomal membrane tubulation (from [54]). (D) Different groups of SNXs have various functions depending on their sequence similarity (from [50]).

Research shows that the Vps26/29/35 subcomplex is not able to interact with membrane lipids directly, but it is recruited to SNX-Bar dimers [56]. How the retromer subcomplex associates with SNX remains unknown, although there is evidence showing that retromer interacts through N-terminal extensions of SNX1 and SNX2 [57,58]. It is also believed that the SNX subcomplex is required for retromer subcomplex recruitment onto membranes by creating a subdomain of the early endosome, which acts as a docking site to recruit the Vps26–Vps29–Vps35 subcomplex [59]. However, SNX alone is not enough to recruit the Vps subcomplex. Other factors

on the endosomes seem also to be crucial for Vps subcomplex recruitment. Research shows that the small GTPase Rab7 is necessary to regulate VPS recruitment onto membranes, and Rab5 also indirectly contributes to the recruitment through phosphatidylinositol 3-kinase (PI3K, a Rab5 effector) activation [60].

Once both the SNX-BAR dimer and Vps trimer are recruited onto the endosomal membranes, the Vps trimer can recognize and bind to certain motifs of the cytosolic domain [51, 60]. L2, as mentioned before, utilizes the WLM-like motifs FYL and YYML, which are located close to the C-terminus, to bind to Vps35 and direct its egress from endosomes [48]. Knock-down of Vps26, Vps29 or Vps35 inhibits HPV16 transport into the TGN [61]. After HPV-containing vesicles leave endosomes, they enter the TGN with the help of gamma-secretase (a membrane associated protease complex) [62], and thus the virus avoids the fate of degradation in host cell lysosomes. However, to establish effective viral infection, viruses still need to find a way to deliver their viral genome into the nucleus. How HPV imports its genome into the nucleus is still unknown, but mitosis is believed to be critical for HPV infection, as the nuclear envelop breaks down and the TGN becomes dispersed, so the virus can access the nucleus [63]. Research has also shown that G1, S, G2 and early M phase cell cycle inhibitors will inhibit virus infection [15]. The virus genome eventually localizes to nuclear structures called promyelocytic leukemia bodies (PML) and PML bodies are required for efficient transcription of the virus genome [64].

Studies with TacL2 chimeras to better understand L2-dependent endocytosis and trafficking and the role of SNX-BAR proteins in HPV infection

More and more evidence suggests HPV can utilize host cell retrograde transport mechanisms to transport its genome to the TGN, thus avoiding lysosomal degradation. In this study we hypothesize that early L2 spanning of the endosome membrane, followed by direct binding and recruitment of cytosolic sorting factors, may contribute to viral endocytosis and subcellular retrograde trafficking of viral DNA towards the TGN. We took a Tac-chimera approach to study L2-dependent trafficking and endocytosis. Upon spanning of the endosomal membrane, sequences downstream of the L2 transmembrane domain are presumably exposed to the cytosol. We fused this intracellular portion of L2 (residues 67-473) with the N-terminal ectodomain and trans membrane domain (TMD) of the Tac protein (CD25/IL-2 receptor), adding an HA tag at the extreme C-terminus (Fig. 3). Transient expression of this TacL2HA chimera enables us to study endocytosis and trafficking with anti-Tac ectodomain antibodies. We also combined this system with a cell surface biotinylation approach to further study L2-dependent endocytosis of the chimera.

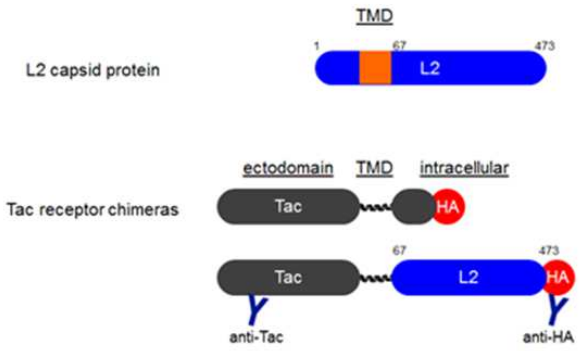

Fig 3. TacHA and TacL2HA constructs. L2 residues 67-473 are fused to the Tac ectodomain and its trans membrane domain (TMD). Both Tac and the TacL2 chimera are attached to an HA tag at their C-terminus. These proteins can be stained by anti-Tac antibody outside of cell membrane and anti-HA inside of membrane.

Retromer-dependent trafficking of cargo from early endosomes to the TGN is known to involve certain members of the sorting nexin family, specifically the SNX-BAR proteins. We also performed a small siRNA screen of the SNX-BAR subfamily proteins and identified SNX6 and SNX32 (aka SNX6b) as SNX-BAR proteins that may be specifically involved in retrograde trafficking of HPV16 L2/vDNA during infection. Future work will focus on the mechanisms through which L2 and SNX6 influence HPV16 entry and trafficking.

Results

TacL2HA chimera has higher internalization efficiency compared to TacHA

In order to investigate if L2 affects endocytosis from the cell surface, we used NHS-SS-biotin to label all cell surface proteins of TacHA-, TacL2HA- and GFP-transfected cells (Fig.4A). For the control groups (GFP and "total" groups, transfected with TacHA or TacL2HA), the cells were washed, lysed, and aliquots were prepared for Western Blot to measure total surface biotinylated TacHA/ TacL2HA levels. For the rest of the experimental groups, their surface proteins were allowed to undergo endocytosis for different amounts of time. Remaining cell surface biotin molecules were then cleaved and washed away using the cell-impermeable reducing agent MESNA, thus only internalized biotin signals to remain. Cells were lysed and aliquots were prepared for western blot. Aliquots were run on SDS-PAGE and western blots were performed, staining with Rat anti-HA to measure total HA signal of both control group and experimental groups (input group, total levels of TacHA or TacL2HA following

transfection). For the remaining lysate samples, we used immobilized neutravidin resin to pull down all the biotinylated proteins, washing away all unbound (no biotin labeled) proteins, and performed western blot, staining with rat anti-HA antibody to detect internalized TacHA or TacL2HA levels (pull down group, only internalized HA signals are detected because MESNA is membrane impermeable and removes only surface-bound biotin). Pull down band intensities were first normalized to input bands, then the percent internalization was calculated and normalized. The ratio represents percentage of internalized TacHA/TacL2 proteins compared with total surface TacHA/TacL2HA level before endocytosis. The western blot bands and normalized TacHA/ TacL2HA internalization level for different endocytosis duration is shown in Fig.5A.

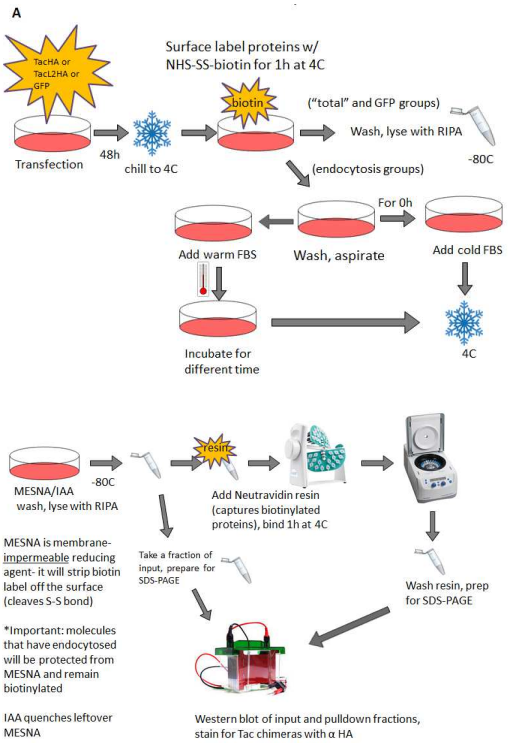

Fig 4. A schematic diagram of biotin pull down experiments. (A) TacHA-, TacL2HA- or GFP-transfected cell surface proteins are labeled by NHS-SS-biotin. For the control plate (GFP group, and total group), the cells were washed and collected to measure total surface HA level. For the experimental group, they undergo endocytosis for different time periods. Then, MESNA is used to cleave and remove all cell surface biotin. Cells are lysed and aliquots taken from the experimental and control plates group. Western Blots are performed with Rat anti-HA to measure total HA levels (input, total levels of TacHA or TacL2HA transfection). For the rest of samples, immobilized neutravidin resin is used to pull down biotinylated proteins and perform western blot, probing with rat anti-HA antibody to detect internalized TacHA or TacL2HA levels (pull down, only internalized HA signals are detected). Any proteins without biotin labeling are washed away by using RIPA washing buffer. (B, following page) A more simplified diagram is shown to demonstrate the basic ideas described above.

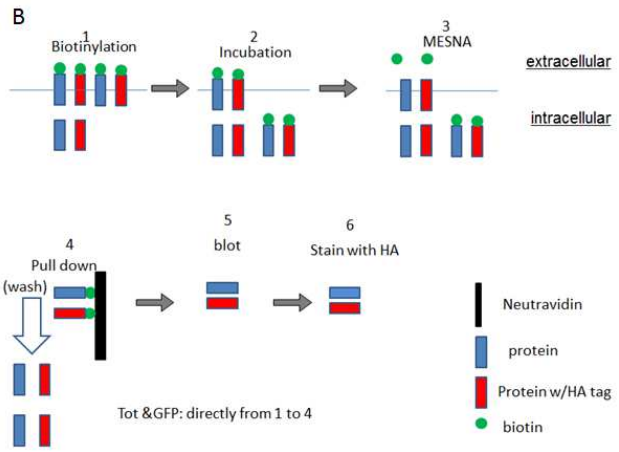

The TacL2HA protein tends to have higher internalization compared with TacHA protein, suggesting that TacL2HA is internalized more efficiently. Alternatively, TacL2HA has slower degradation, suggesting that TacL2HA and TacHA follow different intracellular trafficking pathways. Both factors may contribute to more endocytosed HA level detected in TacL2HA-transfected cells. We also used immunofluorescence staining to verify the observed increase in endocytosis of TacL2HA. Live chimera-expressing cells were first surface stained by Mouse anti-Tac antibody at 4℃ to label all the cell surface TacHA/TacL2HA molecules. Cells were then transferred to 37℃ incubator to allow to internalize for different time periods. Unbound Mouse anti-Tac antibodies were washed away and cells were then fixed, and stained with anti-mouse 488 secondary antibody (green signal). Cells were washed again to remove unbound secondary antibody and then permeabilized and stained with anti-mouse 555 so all the TacHA or TacL2HA proteins are stained by red. In this way the red-only signal represents TacHA or TacL2HA proteins that have been internalized into cells, and were thus protected from the initial anti-mouse 488 stain before

permeabilization. The yellow signal (green plus red) represents the TacHA or TacL2HA proteins remaining on cell surface (Fig.5B). In TacL2HA transfected cells, more internalized TacL2HA signal (red) can be detected after same internalization duration compared to TacHA transfected cells. This is more significant at late time points for endocytosis such as two hours and three hours.

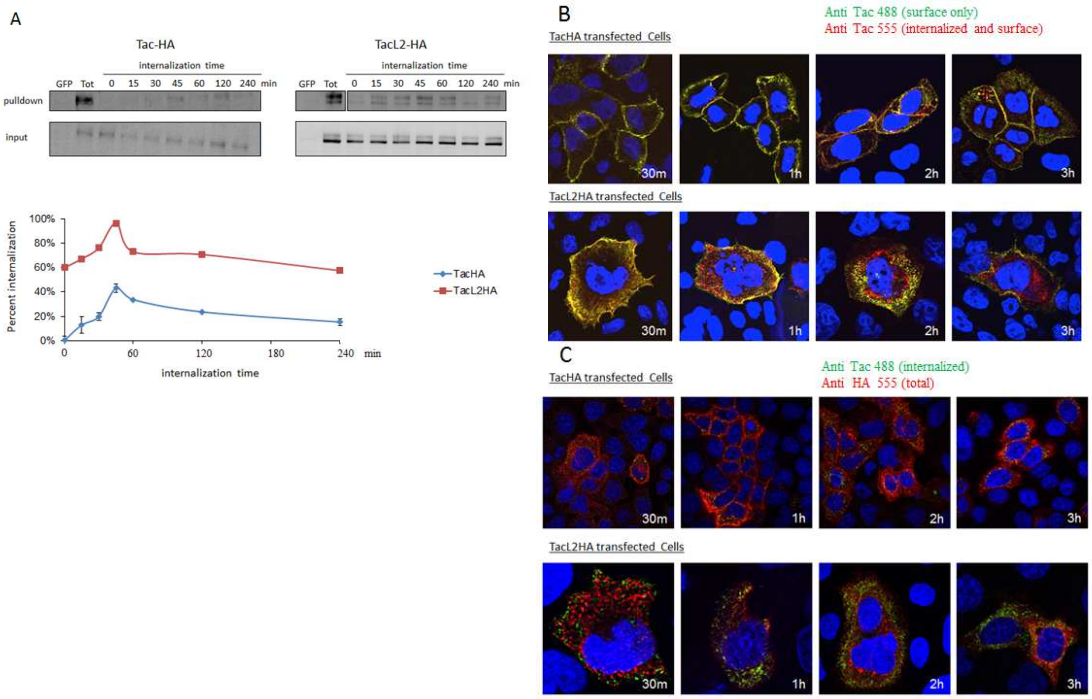

Fig 5. TacL2HA chimera has higher internalization efficiency compared to TacHA . (A) Cell surface proteins are biotinylated as described in Materials and Methods and Figure. 4, then cells are incubated at 37℃ to start internalization. After different duration of incubation, biotin remaining on cell surface is stripped by MESNA, and cells are lysed by RIPA buffer. The internalized biotin lysate is pulled down by neutravidin. A portion of the lysate is collected from each group to perform western blot, staining with Rat anti-HA antibody to detect total expression level in each group. Pulldown bands are first normalized to input bands, then the internalization percentage (divided by normalized total band) is calculated. (B) Cells were first surface stained by Mouse anti-Tac antibody then transferred to 37℃ for different amounts of time to permit internalization. Cell were fixed, stained with anti-mouse 488, and then permeabilized, followed by staining with anti-mouse 555. The yellow signal (green plus red) presents the TacHA or TacL2HA proteins remaining on cell surface. The red signal presents the TacHA or TacL2HA proteins internalized into cells. (C) Cells were first surface stained by Mouse anti-Tac antibody followed by incubation at 37℃. Surface Tac antibody was washed away by acetic buffer. Cells were fixed and stained with rat anti-HA. Then, cells were stained with anti-mouse 488 to identify internalized Tac, and stain with anti-rat 555 to visualize total levels of the chimeras.

To further verify the effects of L2 on endocytosis efficiency of the chimera, we performed another immunofluorescence-based internalization assay. Live chimera-expressing cells were first surface stained by Mouse anti-Tac antibody to label all surface TacHA/TacL2HA proteins. Then, cells were transferred to 37℃ to allow for chimera internalization for different periods of time. After incubation, any remaining surface mouse anti-Tac antibody was washed away by rinsing cells twice with acetic buffer. Acetic buffer was then washed away with a PBS rinse. Cells were then fixed, permeabilized, and stained with rat anti-HA. Secondary stain with anti-mouse 488 was used to identify internalized Tac chimeras (all surface Mouse anti-Tac antibodies are washed away by acetic acid buffer), and stained with anti-rat 555 to identify total chimera levels (Fig.5C). Compared to TacHA transfected cells, there is more endocytosed protein signal (green) in the TacL2HA group. This suggests an important role of L2 sequences in chimera endocytosis. Combined, all three separate assays suggest that L2 residues 67-473 can enhance the efficiency of Tac chimera endocytosis.

TacL2HA chimera follow different intracellular trafficking pathway compared to TacHA

To investigate how the internalized TacL2HA and TacHA proteins traffic in the cells, we used different intracellular markers to identify the internalized protein location. Cells were first surface stained by Mouse anti-Tac antibody and then transferred to 37℃ to permit internalization and trafficking. Surface Tac antibodies were then washed away by acetic buffer and cells were fixed, permeabilized, and stained with antibodies against

proteins that mark intracellular compartments such as rabbit anti-EEA1 (labels early endosome) or rabbit anti-TGN46 (labels *trans*-Golgi network). Cells were then stained with secondary (anti-mouse 488) to identify internalized Tac, and anti-rabbit 555 to stain different intracellular compartments. As seen before, the overall levels of endocytosed TacL2HA (green signal) was much greater than TacHA, again suggesting that L2 sequences can promote endocytosis. Both TacHA and TacL2HA proteins have some colocalization with the early endosome at different time points. This may suggest L2 didn't have significant effects for proteins to traffic into early endosomes (Fig.6A). For the TGN staining, both TacHA and TacL2HA have limited colocalization with TGN at 30 minutes, but at 2 hours there is a dramatic increase of TacL2HA colocalization with TGN, suggesting L2 plays an important role directing protein traffic from endosomes to the TGN (Fig.6B). We also tried to stain with rabbit anti-Vps26 in this experiment. However, after acetic buffer washing, the Vps26 signals were very weak. Therefore, data in Fig.6C was collected without acetic buffer washing. Compared with TacHA transfected cells, TacL2HA transfected cells seem to have higher colocalization level with Vps26 (labels the retromer subcomplex) after either 30 minutes or 2 hours, suggesting retromer may interact with TacL2HA directly after endocytosis and may play an important role during TacL2HA intracellular trafficking.

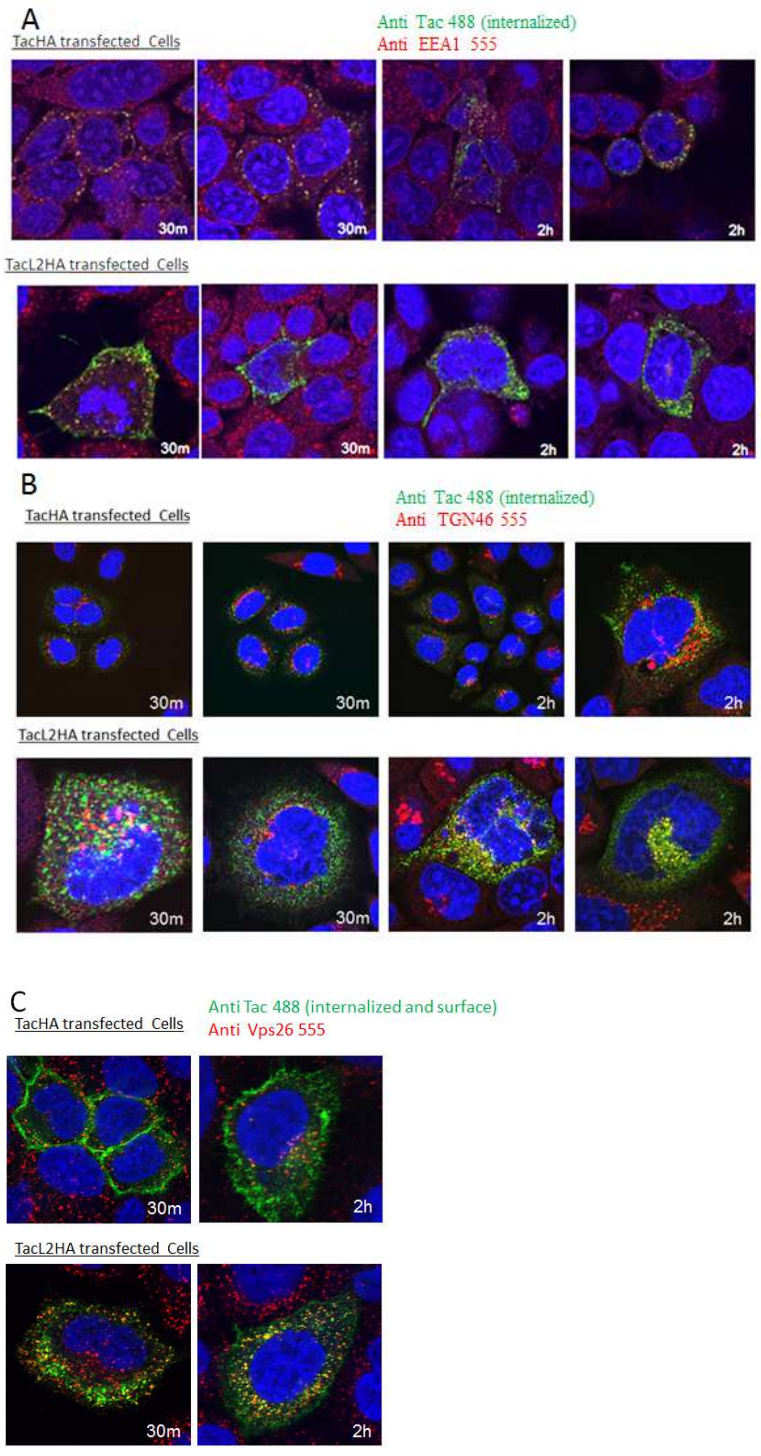

Fig 6. TacL2HA chimera follows different intracellular trafficking pathway compared to TacHA. Cells were first surface stained by Mouse anti-Tac antibody, then transferred to 37 °C, to allow internalization. Surface Tac antibodies were washed away by acetic acid buffer. Cells were fixed and stained with rabbit anti-EEA1 or rabbit anti TGN46. Secondary stain was performed with anti-mouse 488 to identify internalized Tac level, and anti-rabbit 555 to stain different intracellular markers. All cells are at the same magnification but with different zoom in scale. (A) Co-stained with Tac and EEA1. (B) Co-stained with Tac and TGN46. (C) Co-stained with Tac and Vps26.

HPV16 infection efficiency is affected by certain SNXs

To investigate if SNX–BARs family proteins have effects on virus infection, we performed siRNA knockdown for each SNX–BARs family member in HaCaT cells. Knock-down cells were infected with luciferase-expressing pseudovirus to detect virus infection activity by luciferase assays (Fig.7A). All siRNA knockdowns were verified by RT-qPCR (except SNX32) (Fig.7B). SNX6 knockdown was also verified by western blot (Fig.7C). For the SNXs shown in the literature which are involved in endosomal sorting through retromer (SNX1, SNX2, SNX5, SNX6 and SNX32, Figure 2D), we found they have drastically different effects on viral infection.

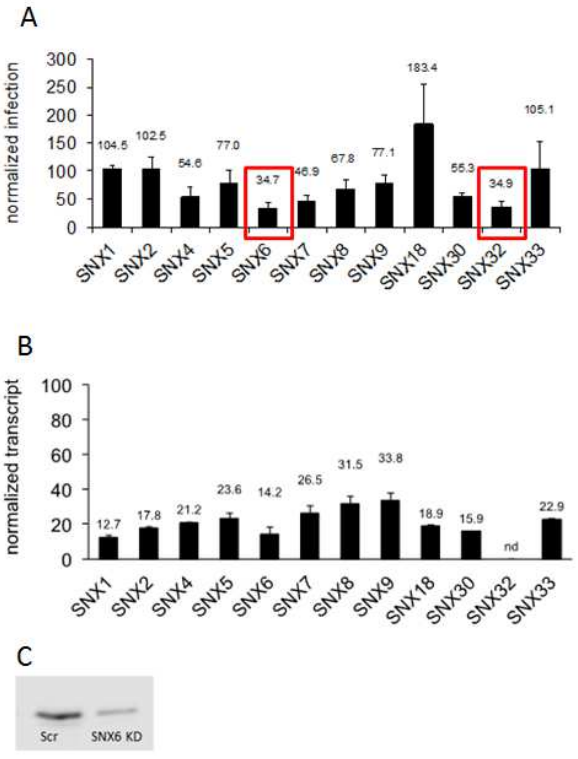

Fig 7. HPV16 infection efficiency is affected by certain SNXs. (A) HaCat cells are transfected by Sorting Nexin siRNA and with control siRNA (Scramble) using Lipofectamine RNAiMAX reagent. 24h after transfection, cells were infected by Pxull WT-Luc virus. After 24 hours of infection, cells were lysed and analyzed by Luciferase assay to quantify virus infection. All knockdown samples were normalized by western blot of GAPDH. (B) The knockdown cells were also collected for RNA extraction to perform RT-qPCR to detect SNX transcript levels. (C) The SNX6 knock down cell lysate is performed western blot method together with Scramble. The blot was stained by mouse anti-SNX6 antibody.

Single knockdown of, and SNX5 had little effects on virus infection, despite their important role in endosomal membrane binding and tubulation induction [57, 76]. In contrast, both SNX6 knockdown and SNX32 knockdown had very strong effects that decrease virus infection. SNX4, SNX7 and SNX30 are supposed to be involveed in endosomal recycling [50]. Interestingly, in addition to SNX4, knocking down SNX7 and SNX30 also decreased virus infection moderately. These SNXs are reported to be involved in endosomal recycling [50]. Knocking down SNX18 increased virus infection dramatically, and SNX18 has been identified as a positive regulator of autophagosome formation [66]. This might suggest host cell may use autophagy pathway to restrict HPV infection.

TacL2HA transfected cells tend to have abnormal cell phenomenon: Golgi fragmentation and multinucleation.

During the TacHA and TacL2HA transfection we found some strange phenomena. After 48 hours of transfection, the TacHA-transfected cells are quite normal and have compact Golgi, but the Golgi of TacL2HA-transfected cells are more dispersed, and they tend to occupy more space in the cytoplasm (Fig.8A). We used the ratio of Golgi area to nuclear area (defined as dispersal index) to quantify this phenomenon. The TacL2HA-transfected cells have a higher average dispersal index and some of them have larger Golgi area compared to nuclear area (Fig.8B). In TacL2HA-transfected cells, there are more nuclei per cells compared to TacHA transfected cells (Fig.8C). Some of them even have more than 5 nuclei in a single cell. During mitosis the Golgi is

dispersed, partitioned into daughter cells, and is later reorganized after cell division. The mitotic chromosomes also segregate into daughter cells.

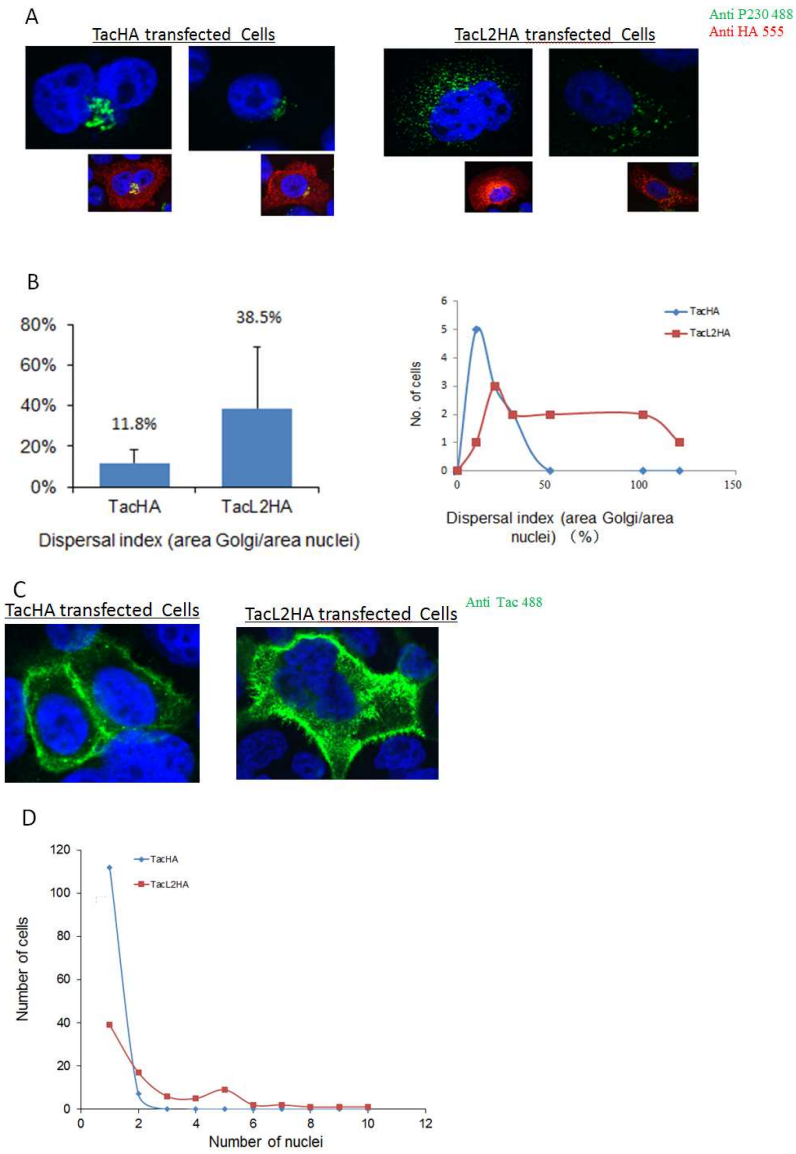

Fig 8. TacL2HA transfected cells tend to have abnormalities: Golgi fragmentation and multinucleation. (A) For the Golgi Fragmentation experiments, cells were fixed, permeabilized and stained with mouse anti-p230 followed by Alexa Fluor 488-conjugated donkey anti-mouse IgG, and rat anti-HA followed by Alexa Fluor 555-conjugated donkey anti-rat IgG. Slides were imaged using a confocal microscope. (B) Both the area of Golgi and area of nuclei are circled and calculated and their ratio is defined as the dispersal index. (C) For the multinucleation experiments, cells were stained by mouse anti-Tac followed by Alexa Fluor 488-conjugated donkey anti-mouse IgG. The nucleus number was counted in each single cell and if the nucleus number was difficult to determine, then the smallest possible number was used.

Sustained Golgi fragmentation and multinucleation phenomenon may imply the TacL2HA transfected cells undergo some mitotic defect, and L2 appears to play a role in such phenomenon. Future work is required to investigate if L2 can affect the process of cellular mitosis.

Discussion

Although a lot of work has been done on HPV binding and subcellular trafficking, the mechanisms of virus infection are still unclear and a lot of data remains controversial. L1 is crucial in initial virus binding and encapsidation, but binding of L1 to heparin sulfate proteoglycan (HSPG) alone could not mediate efficient virus endocytosis, suggesting L2 could play an important role for virus internalization [40]. Binding of HPV to HSPG will cause capsid conformational changes mediated by cyclophilin B (CyPB), allowing more L2 protein N-terminus exposure [41]. On the L2 N-terminus there is a highly conserved furin convertase site (9-RTKR-12), which can be cleaved by furin. In this study we hypothesize that L2 plays an important role for virus egress from the endosome and trafficking to the TGN, maybe through its membrane spanning and recruitment of host sorting factors such as certain SNXs. This spanning may happen very early after entry or even on the surface before endocytosis and may require furin cleavage to adopt the spanning conformation. Research shows that L2 fails to reach the Golgi when furin cleavage is blocked [72].

Because it is difficult to use native virus to study HPV biology, we use virus-like particles (VLP) and the TacL2HA chimera to study L2 function during virus infection.

Both the biotin pull-down experiments and surface Tac immunofluorescence experiments show that L2 can enhance endocytosis efficiency. After TacHA or TacL2HA chimera get endocytosed into the cell, they seem to follow different intracellular trafficking pathways. The TacL2HA chimera has high colocalization with TGN46, and TacHA protein has little colocalization to TGN46, suggesting L2 may contribute directing protein egress from endosome and trafficking into the TGN. The most well-known protein trafficking pathway from endosome to Golgi is the retrograde pathway, and retromer is one of the most important components to perform this function by selecting cargo and recruiting a motor complex on the endosomal membrane, followed by trafficking towards the TGN. At late time points there is significant colocalization of TacL2HA with Vps26, suggesting it may interact directly with retromer. It is not surprising for the virus to hijack host cell trafficking pathways for its own benefit. Since studies have shown that L2 can span through the endosomal membrane, we hypothesize that L2 can bind to retromer and mediate transport of the virus genome to the TGN, thereby avoiding lysosomal degradation.

Studies showed that knock down of certain Vps proteins can affect virus transport from endosome to TGN [61], but the importance of SNX-BAR family proteins during HPV infection still needs to be determined, and we know they can cause membrane curvature and bind to and induce endosomal membrane tubulation, which is an important endosomal cargo selection platform. N-terminal extensions of SNX1/SNX2 can interact with Vps, and it can also bind to or induce endosomal membrane tabulation [59]. Thus SNX1 and SNX2 are thought to be important during retrograde transport.

Research also show SNX1/SNX2 is crucial in retrograde transport of CI-MPR together with SNX6 [59]. We performed a SNX-BAR siRNA knockdown experiment and found that SNX6 and SNX32 both have strong effects on virus infection. However, despite the fact that they are main retromer partners for endosome to TGN traffic, SNX1, SNX2 or SNX5 alone have little effects on virus infection.

We found that knock down of SNX18 can increase virus infection. SNX18 was identified as a positive regulator of autophagosome formation [66]. Because autophagosome is the intracellular organelle that capable to deliver cytoplasmic contents and invading microorganisms into the lysosome for degradation [75], it maybe suggest host cell may use autophagy pathway for HPV degradation, thus restrict HPV infection.

After HPV is transported into the Golgi, it must find a way to get access to the host cell nucleus. There is no evidence showing L2 can cause nuclear envelope disruption directly, and it is more likely that the virus must wait for cell to disassemble the nuclear envelop during mitosis and then traffic into nucleus and replicate. During TacL2HA transfection, we found that the Golgi of host cells seems to be more dispersed and there are multiple nuclei in single cells. This suggests that TacL2HA causes some mitosis defects, and this may or may not relate to virus translocation into cell nucleus.

Future research should focus on looking for evidence to show direct interaction between L2 and SNXs. We know that knocking down certain SNXs such as SNX6 and SNX32 will affect virus infection dramatically, and if we can find evidence showing SNX6 or SNX32 interact with TacL2HA chimera directly, but not with TacHA, added

together with our TGN46 and VPS26 TacL2HA colocalization immunofluorescence results, then this may contribute to our model that HPV can hijack host cell retrograde mechanisms to traffic into the TGN, mediated by host cell retromer composed of Vps trimer and certain SNX dimers, such as SNX6 and SNX32.

If we found direct evidence for L2/SNX6 and SNX32 interaction, the next step is to identify how such interaction occurs. Does L2 bind to SNX6 directly (and what are the domains and residues involved), or does it interact with SNX6 indirectly through Vps? These questions can be addressed through mutagenesis of L2.

Another question is whether SNX affect virus endocytosis directly. The mechanism of virus endocytosis is still poorly understood. There are controversial data showing different possible mechanisms, and maybe SNX also plays a role in virus endocytosis. We found a subfamily of SNX-BAR family (SNX4, SNX7 and SNX30) proteins that have moderate effects on virus infection, and they are supposed to be involved in endosomal recycling to return vesicles to cell surface [50]. It may imply the host endosomal recycling pathway can contribute to virus egress from endosome, but it is also likely to contribute to viral infection in an indirect way. We hypothesize that if we knock down those SNXs involved in endosomal recycling, then the pathway of certain surface molecules returning back to cell surface membrane may be restricted, and those molecules may play important roles during viral endocytosis towards endosome. So, these SNXs may contribute to virus infection through endocytosis, if not through egress from endosome by retrograde transport. To verify this we may need to knock down the SNXs that involve in endosomal recycling, and then investigate the endocytosis

efficiency of VLPs. For example, we may try to repeat the surface biotin-labeled endocytosis experiments in SNX (those involved in endosomal recycling) knockdown cells. If we do find difference of endocytosis efficiency, then it may suggest certain SNXs are important for viral endocytosis. Additionally, it may be also necessary to identify which cellular membrane molecule is important for endocytosis efficiency.

Finally, it may be helpful to investigate the relationship between TacL2HA and strange Golgi dispersal and polynucleation phenotype because they may relate to cell mitosis deficiency. We don't know which part on L2 downstream sequence is responsible for the Golgi dispersal phenomenon and polynucleation phenotype. We could perform mutagenesis of L2 combined with immunofluorescence (IF) staining for Golgi and nucleus to identify these regions. If the deletion of certain sequence on TacL2HA chimera will lead to the transfected cells undergo normal cell cycle without the abnormal Golgi dispersal and polynucleation phenomenon, then we may conclude that certain sequence on L2 is responsible for cell mitosis deficiency on TacL2HA transfected cells. We can also check whether the viral trafficking is affected if the strange Golgi dispersal and polynucleation phenotype disappeared. Will the viral endocytosis efficiency get affected? Or will the retrograde trafficking get inhibited? Or it just induces abnormal Golgi dispersal and polynucleation phenomenon but has no effects on viral trafficking?

It may be also important to identify which cellular factor is interacting with such sequence of L2. We could attempt an siRNA knockdown screen of cellular proteins to see if anything prevents the strange phenotypes observed with TacL2-HA transfection.

Alternatively, we could attempt to identify these L2-interacting proteins by pull down experiment. If we can pull down certain cellular factors (such as SNX6 or SNX32) together with TacL2HA chimera, but cannot pull down with the mutated TacL2HA chimera (that induces no abnormal Golgi dispersal and polynucleation phenomenon), then those cellular factors may be also involved in abnormal Golgi dispersal and polynucleation. If those cellular factors can be identified, then we may try to knock down them and transfect cells with normal TacL2 HA chimera to see if the abnormal Golgi dispersal and polynucleation phenomenon decreased. If yes, then the cellular pathways that involve these factors may be crucial for abnormal Golgi dispersal and polynucleation phenomenon. For example, if we knock down SNX6 or SNX32 and the abnormal Golgi dispersal and polynucleation phenomenon decreased, then this may suggest the cellular retrograde trafficking pathway is required or upstream of the abnormal Golgi dispersal and polynucleation phenomenon.

Materials and methods

Cell culture.

HaCaTs cells (an immortal human keratinocyte cell line) were maintained in high-glucose cDMEM media supplemented with 10% fetal bovine serum (FBS) and antibiotic/antimycotic (Bio5 Institute Media Facility). Hela cells were maintained in high-glucose cDMEM media supplemented with 10% bovine growth serum (BGS) and antibiotic/antimycotic (Bio5 Institute Media Facility). Both cell lines were kept in 37℃ incubator with 5% CO_2.

TacHA and TacL2HA plasmids.

Chimera L2 protein was made by transmembrane domain (TMD) downstream sequence of L2 fused with ectodomain and trans membrane domain of Tac protein (Il-2 receptor), which is a cell surface protein. The Tac-L2 was also fused with a HA tag at its end. Tac protein is attached by HA tag at its intracellular end for control. Both proteins can be stained by mouse anti-Tac antibody from outside of cell membrane or stained by anti-HA inside of cell membrane (Fig.3)

TacHA and TacL2HA surface internalization efficiency, surface biotinylation and pull down experiment

Hela cells were grown on 6-well plates and transfected by TacHA, TacL2HA, and GFP plasmids using Lipofectamine 2000 reagent (Invitrogen) for 48 hours. Cells were cooled to 4℃ for 20 minutes to stop surface protein endocytosis. Then cells were washed 3 times with washing buffer (1x PBS, pH=7.5 with Mg 2+, Ca 2+). The plasma membrane proteins were biotinylated in washing buffer containing 1.5 mg/mL Sulfo-NHS-SS biotin (Thermo) for 1 hour. Cells were washed with 1 time quenching buffer (100 mM glycine in PBS buffer) to remove excess free biotin and wash 2 times washing buffer. For the control plate (GFP group and no MESNA washed TacHA/ TacL2HA group, the total group), the cells were added 500 ul cold lysis buffer (490 ul RIPA, 5ul PMSF, 5ul protein inhibitor), swirl to cover cells, freeze plate at -80℃ overnight. For the experiment plates, they were put in 37℃ incubator and incubate for 0, 15m, 30m, 45m, 1 h, 2h, 4h to allow biotinylated surface protein endocytosis.

After each time points the cells were quickly cooled to 4℃, and all biotinylated proteins remaining on cell surface were stripped by three times 15 minutes washes in MESNA (Sigma) stripping buffer (75 mM 2-mercaptoethanesulfonic acid, 150 mM NaCl, 1 mM EDTA, 0.2% BSA, and 20 mM Tris, pH 8.6). Then wash away excess MESNA by three 5 minutes washes in iodoacetamide (IAA. Sigma) buffer (50 mM iodoacetamide in PBS). The cells were added 500 uL cold lysis buffer (1% PMSF and 1% protein inhibitor in RIPA), swirl to cover cells, freeze plate at -80℃ overnight. Thaw all plates on ice and transfer lysate to microfuge tubes. Spin down at 10000g for 5 minutes in 4℃. Collect supernatant into new tubes. Take part of both experiment group and control group lysate and elute them in sodium dedecyl sulfate1 (SDS1) buffer (0.5M Tris, glycerol, 10%SDS, 2-mercaptoethanol and 1% bromophenol blue) and perform western blot methods described below. Stain with rat anti-HA antibody and anti-rat 800 to measure HA transfection level of each group (input). For the rest lysates, add 15 ul neutravidin resin, mix by inversion on shaker, Bind for 3h at 4℃, spin down at 2500g for 2m, discard supernatant, add RIPA lysis buffer (50mM tris-HCL PH=8.0, 150mM NaCl, 0.5 Na-deoxycholate, 0.5% SDS. Bio5 Institute Media Facility) into tubes, vortex and set on ice for 5m, spin down at 2500g for 2m, and discard supernatant again. Repeat RIPA washing 3 times and wash 1 time 1x PBS, discard supernatant and dilute pellet with SDS1, PBS, PMSF, protein inhibitor solution. Perform western blot, stain with rat anti-HA antibody and anti-rat 800 to measure biotin-labeled TacHA/TacL2HA signal (pull down). Pull down band intensities were first normalized

to input bands, then calculate percent internalization (divide by normalized total). The ratio shows percentage of internalized TacHA/TacL2HA at different time points.

TacHA and TacL2HA surface internalization efficiency, two different secondary antibody staining for Tac antibody.

Hela cells were plated on 6-well plates and transfected by TacHA and TacL2HA plasmids using Lipofectamine 2000 reagent (Invitrogen) for 24 hours, then transfer them into 24 well plates for another 24 hours growth. After 48h transfection cells were placed in 4℃ for 20 minutes to stop cell surface protein internalization. Cells were washed 3 times with cold PBS and surface stain with mouse anti-Tac (Catalog # 05-170) antibody (1:500 in 200 ul FBS) for 1h at 4℃. Wash with 1x PBS, add warm FBS and put in 37℃ incubator to allow internalization for different time points. After incubation, chill cells and fix by PFA fixation buffer for 10 minutes, stain with anti-mouse 488 (1:1000 in 80% PBS and 20% blocking buffer) for 1h at RT. Then wash with 3 times PBS, permeabilize with permeabilization buffer, stain with anti-mouse 555 (1:1000 in 80% PBS and 20% blocking buffer) for 1h at room temperature. Wash with 3 times PBS, prepare the slides and check by confocal microscope.

TacHA and TacL2HA surface internalization efficiency, acetic acid wash for cell surface Tac antibody.

Hela cells were plated on 6-well plates and transfected by TacHA and TacL2HA plasmids using LipofectAMINE 2000 reagent for 24 hours, then transfer them into 24

well plates for another 24 h growth. After 48h transfection cells were placed in 4℃ for 20 minutes to stop cell surface protein internalization. Then cells were washed 3 times with cold PBS and surface stain with mouse anti-Tac antibody (1:500 in 200 ul FBS) for 1h at 4℃. Wash with PBS, add warm FBS and put in 37℃ incubator to allow surface internalization for different time points. After incubation, chill cells and wash with 2 time PBS, 2 times acetic acid buffer (0.5 M NaCl, 0.5% acetic acid, pH=2.4), 2.5 minutes each time (wash away any mouse anti-Tac antibody binds to surface Tac), then wash 3 times PBS. Fix by fixation buffer for 10 minutes, stain with rat anti-HA (1:400 in 80% PBS and 20% blocking buffer) 1h at room temperature (detects total Tac transfection level). Wash 3 times of PBS, secondary stain with anti-mouse 488 (1:1000 in 80% PBS and 20% blocking buffer, for internalized Tac), and anti-rat 555 (1:1000 in 80% PBS and 20% blocking buffer). Wash with 3 times PBS, prepare slides by adding anti-fade mounting medium with DAPI (Life technologies) and check by confocal microscope.

TacHA/TacL2HA internalization and colocalization with intracellular markers

The experiment method is the same as the acetic acid wash experiment described above except the primary antibody is replaced by rabbit anti-TGN46 (Sigma. 1:400 in 80% PBS and 20% blocking buffer), rabbit anti-EEA1 (Cell Signaling. 1:400 in 80% PBS and 20% blocking buffer) and rabbit anti Vps 26 (abcam. 1:400 in 80% PBS and 20% blocking buffer). The secondary antibody is replaced by anti-rabbit 555 with same concentration.

Sorting nexin knockdown

35000 HaCaT cells were plated on 24-well plates in SiRNA media（high-glucose cDMEM supplemented with 10% FBS, antibiotics-free. Bio5 Institute Media Facility）. Replace media with 1x Opti-MEM reduced serum medium（life technologies）in each well and add different SNX SiRNA-lipofectamine complex and control SiRNA-lipofectamine complex. 16h after transfection, wash with 1x PBS and replace with SiRNA media.

Luciferase assay

24h after performing sorting nexin knockdown protocol, cells were infected by Pxull WT-Luc virus (2E8 viral genome equivalents in 500 ul SiRNA media). After 24 hours of infection, cells are washed by PBS and treated with 100 ul 1x RLB for 5 minutes at room temperature and then freeze in -80℃ overnight. Thaw plates on ice and collect lysate into tubes, add 10 ul sample lysate into 96 well white microtiter plate and add 50 ul Luciferase assay reagent (LAR. Promega) into each well. Then turn on DTX800 multimode plate reader to record luciferase activity. The remaining samples are performed western blot and stained with GAPDH (cell signaling) to normalize the Luciferase activity.

RNA extraction and qPCR of SNX knockdown cells

24h after performing sorting nexin knockdown protocol, cells were washed by 1x PBS, and lysed by 200ul RLT buffer (1% beta-mercaptoethanol added), transfer to a gDNA Eliminator spin column to remove genomic DNA. Centrifuge for 30s at 8000g, collect flow through and add 1 volume 70% ethanol and mix. Transfer to RNeasy spin column, centrifuge and discard flow-through. Add buffer RW1, centrifuge and discard flow-through. Add buffer RPE, centrifuge and discard flow-through. Add 50ul RNase free water into tube, centrifuge and collect flow-through. For the RNA sample, add 5ul 10x TURBO DNase buffer and 1 ul DNase to each tube, incubate at 37℃ for 25 minutes. Add 5 ul resuspended DNase inactivation reagent and mix twice during 5 minutes incubation. Centrifuge at 12500 rpm for 1.5 minutes, collect 45 ul RNA supernatant. Dilute purified RNA into same concentration and reverse transcribe them by using high-capacity cDNA Reverse Transcription kit (Thermo fisher Scientific) add 10 ml diluted RNA into 10 ml master mix. Incubate at 25℃ for 25 minutes, 37℃ for 2 hours, 85℃ for 5 minutes to terminate reaction. Use Maxima SYBR Green qPCR master Mix (Thermo Fisher Scientific) for qPCR amplification. The SNX transcription level was detected by Rotor Gene Q qPCR machine (Qiagen) and data was analyzed by using Rotor Gene Q Series Software. The SNX sequences are listed below:

SNX1 primer sequence: 124 (length), AAGCACTCTCAGAATGGCTTC (forward), CGGCCCTCCGTTTTTCAAG (reverse)

SNX2 primer sequence: 139 (length), GGGAAGCCCACCGACTTTG (forward), GGCCATTGGAGTTTGCACTAATA (reverse)

SNX4 primer sequence: 99 (length), AGCAGAAAAACGAACTGGAAGA (forward), CTCTGACCATCGGTATGTTCAAC (reverse)

SNX5 primer sequence: 113 (length), TCTGTATCTGTGGACCTGAATGT (forward), GTGGGCAGTGTGGTCTTTGT (reverse)

SNX6 primer sequence: 324 (length), TTTCTTTGAGCACGAACGAACA (forward), GACCTAGACCTTCGATACAGGAG (reverse)

SNX7 primer sequence: 108 (length), ACTAAGACATCTCGTGGGGAA (forward), CAGAGTGGGGTGTGCTTCTTC (reverse)

SNX8 primer sequence: 122 (length), TACAGACGGTACAATGACTTCGT (forward), GCCTCGATGAACTCCCTGTC(reverse)

SNX9 primer sequence: 144 (length), ACCAAGGCTCGGGTTATGTAT (forward), CCCTCGTTCTCCTTTGATGTTT (reverse)

SNX18 primer sequence: 133 (length), AACCCCTACCCGTTCCAGT (forward), AGTGCTTGTAGCGCCGATG

SNX30 primer sequence: 167 (length), AGCTTCGGTGACAAGGATCTC (forward), CACACATGCTTCTTGGGATCAT (reverse)

SNX32 primer sequence: 128(length), GAGCGGGACAAGGTGAAATTC (forward), TCATTCTCCACGTAGGCATCA (reverse)

SNX33 primer sequence: 106 (length), AGATCGCTGAGACATACTCCAT (forward), TTGGTCTGTTTTGTGGGGTCC (reverse)

Golgi fragmentation and multinucleation phenomenon analysis

Hela cells were plated on 6-well plates and transfected by TacHA and TacL2HA plasmids using Lipofectamine 2000 reagent for 24 hours, then transfer them into 24 well plates for another 24 h growth. Cells are performed with standard immunofluorescence staining methods. For the Golgi Fragmentation experiment, cells are stained by mouse anti-P230 (No.611280. 1:500 in 80% PBS and 20% blocking buffer), rat anti-HA (1:500 in 80% PBS and 20% blocking buffer), wash, stained by anti-mouse 488 (1:1000), anti-rat 555 (1:1000). Slides are imaged by confocal microscope. Both the area of Golgi and area of nuclei are circled and calculated and their ratio is defined as dispersal index. For the multinucleation experiment, cells are stained by mouse anti-Tac antibody (1:500 in 80% PBS and 20% blocking buffer), wash, stained by anti-mouse 488 (1:1000). The nuclei number is counted and if the nuclei number is difficult to determine, then we use the smallest possible number to indicate its nuclei number.

Western blot

For biotin pull down experiments and luciferase assay experiments, samples were lysed in 1x RIPA lysis buffer or 1x RLB (Reporter Lysis Buffer, Promega) supplemented with 1% PMSF and 1% Proteinase inhibitor cocktail (Sigma) mixed with 20% SDS-PAGE denaturing/reducing loading buffer (0.5M Tris, glycerol, 10%SDS, 2-mercaptoethanol and 1% bromophenol blue). Samples were vortexed and incubated for 5 min at 95°C. Same volume samples were loaded in 12.5% polyacrylamide gels for 2h at 100V in Gel running buffer (1X Tris-Glycine-SDS, Bio5 Institute Media Facility).

Samples were transferred to nitrocellulose membrane by using 1x western transfer buffer (0.25M Tris, 1.92M Glycine. Bio5 Institute Media Facility) supplemented with 10% methanol for 1h15m at 0.3A in cold room, and the membrane was blocked in 5% non-fat milk diluted in 1x Tris-buffered saline–Tween (TBST, 200mM Tris, 1.5M NaCl, 1% Tween20, pH=7.5. Bio5 Institute Media Facility) plus 5% milk overnight at 4℃. The blocked membrane was stained with primary and secondary antibodies and was scanned by an Odyssey scanner.

Immunofluorescence staining and confocal microscopy.

Samples staining vary and were described as above. Samples were fixed by fixation buffer (2% paraformaldehyde in PBS) for 10 min at room temperature, wash 3 times by PBS, permeabilized by Permeabilization buffer (0.2% Triton X-100 in PBS) for 7 min at room temperature. After 3 times washing, samples were then blocked in blocking buffer (4% BSA and 1% goat serum in PBS) at 4℃ overnight before performing immune-staining protocol as described above. The Slides were examined on Zeiss inverted microscope with a 63× objective. Confocal imaging is performed and analyzed by Zeiss LSM 510 system. The laser settings used include 405 nm, 488 nm, and 543 nm laser. Laser intensity was adjusted to bright enough but not to oversaturate. Multiple focal planes are imaged during single stacking on one field.

Acknowledgements

The author would like to acknowledge Dr. Paul St. John, Dr. Campos, Dr. Lybarger, Dr. Elliott and Dr. Harris for their invaluable input and advice in preparation of this thesis.

References

1. Baker, T. S., W. W. Newcomb, N. H. Olson, L. M. Cowsert, C. Olson, and J. C. Brown. 1991. Structures of bovine and human papillomaviruses. Analysis by cryoelectron microscopy and three dimensional image reconstruction. Biophys. J. 60:1445-1456.

2. Zaravinos A. An updated overview of HPV-associated head and neck carcinomas. Oncotarget. 2014;5(12):3956-69.

3. Mistry N, Wibom C, Evander M. Cutaneous and mucosal human papillomaviruses differ in net surface charge, potential impact on tropism. Virol J. 2008;5:118.

4. Bernard HU, Burk RD, Chen Z, van Doorslaer K, Hausen H, de Villiers EM. Classification of papillomaviruses (PVs) based on 189 PV types and proposal of taxonomic amendments. Virology 2010;401(1):70–9.

5. Doorbar J, Quint W, Banks L, Bravo IG, Stoler M, Broker TR, Stanley MA. The

biology and life-cycle of human papillomaviruses. Vaccine. 2012;30 Suppl 5:F55-70.

6. Walboomers JMM, Jacobs MV, Manos MM, Bosch FX, Kummer JA, Shah KV, Snijders PJ, Peto J, Meijer CJ, Muñoz N. Human papillomavirus is a necessary cause of invasive cervical cancer worldwide. J Pathol 1999, 189:12-19.

7. Major T, Szarka K, Sziklai I, Gergely L, Czeglédy J. The characteristics of human papillomavirus DNA in head and neck cancers and papillomas. J Clin Pathol 2005;58(1):51–5.

8. Roden RB, Kirnbauer R, Jenson AB, Lowy DR, Schiller JT: Interaction of papillomaviruses with the cell surface. J Virol 1994, 68:7260-7266.

9. Evander M, Frazer IH, Payne E, Qi YM, Hengst K, McMillan NA. Identification of the alpha6 integrin as a candidate receptor for papillomaviruses. J Virol 1997, 71:2449-2456.

10. Buck CB, Cheng N, Thompson CD, Lowy DR, Steven AC, Schiller JT, Trus BL. Arrangement of L2 within the papillomavirus capsid. J Virol. 2008; 82:5190–5197.

11. Conway MJ, Meyers C. Replication and assembly of human papillomaviruses. J

Dent Res. 2009; 88(4):307-17.

12. Bergant marušič M, Ozbun MA, Campos SK, Myers MP, Banks L. Human papillomavirus L2 facilitates viral escape from late endosomes via sorting nexin 17. Traffic. 2012; 13(3):455-67.

13. Florin L, Becker KA, Lambert C, Nowak T, Sapp C, Strand D, Streeck RE, Sapp M. Identification of a dynein interacting domain in the papillomavirus minor capsid protein l2. J Virol. 2006;80(13):6691-6.

14. Schiller JT, Day PM, Kines RC. Current understanding of the mechanism of HPV infection. Gynecol Oncol 2010;118(1 Suppl):S12–7.

15. Pyeon D, Pearce SM, Lank SM, Ahlquist P, Lambert PF. Establishment of human papillomavirus infection requires cell cycle progression. PLoS Pathog 2009;5(2):e1000318.

16. Wilson VG, West M, Woytek K, Rangasamy D. Papillomavirus E1 proteins: form, function, and features. Virus Genes. 2002;24(3):275-90.

17. Steger G, Corbach S. Dose-dependent regulation of the early promoter of human papillomavirus type 18 by the viral E2 protein. J Virol. 1997;71(1):50-8.

18. McBride AA. Replication and partitioning of papillomavirus genomes. Adv Vir Res 2008;72:155–205.

19. Doorbar J. Molecular biology of human papillomavirus infection and cervical cancer. Clin Sci (Lond) 2006;110(5):525–41.

20. Bodily J, Laimins LA. Persistence of human papillomavirus infection: keys to malignant progression. Trends Microbiol. 2011;19(1):33-9.

21. Münger K, Baldwin A, Edwards KM, et al. Mechanisms of human papillomavirus-induced oncogenesis. J Virol. 2004;78(21):11451-60.

22. Middleton K, Peh W, Southern S, Griffin H, Sotlar K, Nakahara T, El-Sherif A, Morris L, Seth R, Hibma M, Jenkins D, Lambert P, Coleman N, Doorbar J. Organization of human papillomavirus productive cycle during neoplastic progression provides a basis for selection of diagnostic markers. J Virol. 2003;77(19):10186-201.

23. Bedell MA, Hudson JB, Golub TR, Turyk ME, Hosken M, Wilbanks GD, Laimins LA. Amplification of human papillomavirus genomes in vitro is dependent on epithelial differentiation. J Virol. 1991;65(5):2254-60.

24. Stanley M. Immunobiology of HPV and HPV vaccines. Gynecol Oncol. 2008;109(2 Suppl):S15-21.

25. Scott M, Nakagawa M, Moscicki AB. Cell-mediated immune response to human papillomavirus infection. Clin Diagn Lab Immunol. 2001;8(2):209-20.

26. Tindle RW. Immune evasion in human papillomavirus-associated cervical cancer. Nat Rev Cancer. 2002;2(1):59-65.

27. Vambutas A, Devoti J, Pinn W, Steinberg BM, Bonagura VR. Interaction of human papillomavirus type 11 E7 protein with TAP-1 results in the reduction of ATP-dependent peptide transport. Clin Immunol. 2001;101(1):94-9.

28. Hasan UA, Bates E, Takeshita F, Biliato A, Accardi R, Bouvard V, Mansour M, Vincent I, Gissmann L, Iftner T, Sideri M, Stubenrauch F, Tommasino M. TLR9 expression and function is abolished by the cervical cancer-associated human papillomavirus type 16. J Immunol. 2007;178(5):3186-97.

29. Nees M, Geoghegan JM, Hyman T, Frank S, Miller L, Woodworth CD. Papillomavirus type 16 oncogenes downregulate expression of interferon-responsive genes and upregulate proliferation-associated and NF-kappaB-

responsive genes in cervical keratinocytes. J Virol. 2001;75(9):4283-96.

30. Woodman CB, Collins SI, Young LS. The natural history of cervical HPV infection: unresolved issues. Nat Rev Cancer. 2007;7(1):11-22.

31. Zur hausen H. Papillomavirus infections--a major cause of human cancers. Biochim Biophys Acta. 1996;1288(2):F55-78.

32. de Martel C, Ferlay J, Franceschi S, et al. Global burden of cancers attributable to infections in 2008: A review and synthetic analysis. Lancet Oncology 2012; 13(6):607-615.

33. Crook T, Tidy JA, Vousden KH. Degradation of p53 can be targeted by HPV E6 sequences distinct from those required for p53 binding and trans-activation. Cell. 1991;67(3):547-56.

34. Oh ST, Kyo S, Laimins LA. Telomerase activation by human papillomavirus type 16 E6 protein: induction of human telomerase reverse transcriptase expression through Myc and GC-rich Sp1 binding sites. J Virol. 2001;75(12):5559-66.

35. Yim EK, Park JS. The role of HPV E6 and E7 oncoproteins in HPV-associated cervical carcinogenesis. Cancer Res Treat. 2005;37(6):319-24.

36. Williams VM, Filippova M, Soto U, Duerksen-hughes PJ. HPV-DNA integration and carcinogenesis: putative roles for inflammation and oxidative stress. Future Virol. 2011;6(1):45-57.

37. Alazawi W, Pett M, Arch B, Scott L, Freeman T, Stanley MA, Coleman N. Changes in cervical keratinocyte gene expression associated with integration of human papillomavirus 16. Cancer Res. 2002;62(23):6959-65.

38. Jeon S, Allen-hoffmann BL, Lambert PF. Integration of human papillomavirus type 16 into the human genome correlates with a selective growth advantage of cells. J Virol. 1995;69(5):2989-97.

39. Ziegert C, Wentzensen N, Vinokurova S, Kisseljov F, Einenkel J, Hoeckel M, von Knebel Doeberitz M. A comprehensive analysis of HPV integration loci in anogenital lesions combining transcript and genome-based amplification techniques. Oncogene. 2003;22(25):3977-84.

40. Giroglou T, Florin L, Schäfer F, Streeck RE, Sapp M. Human papillomavirus infection requires cell surface heparan sulfate. J Virol. 2001;75(3):1565-70.

41. Bienkowska-haba M, Patel HD, Sapp M. Target cell cyclophilins facilitate human

papillomavirus type 16 infection. PLoS Pathog. 2009;5(7):e1000524.

42. Day PM, Lowy DR, Schiller JT. Heparan sulfate-independent cell binding and infection with furin-precleaved papillomavirus capsids. J Virol. 2008;82(24):12565-8.

43. Smith JL, Campos SK, Wandinger-ness A, Ozbun MA. Caveolin-1-dependent infectious entry of human papillomavirus type 31 in human keratinocytes proceeds to the endosomal pathway for pH-dependent uncoating. J Virol. 2008;82(19):9505-12.

44. Dabydeen SA, Meneses PI. The role of NH4Cl and cysteine proteases in Human Papillomavirus type 16 infection. Virol J. 2009;6:109.

45. Bienkowska-haba M, Williams C, Kim SM, Garcea RL, Sapp M. Cyclophilins facilitate dissociation of the human papillomavirus type 16 capsid protein L1 from the L2/DNA complex following virus entry. J Virol. 2012;86(18):9875-87.

46. Bronnimann MP, Chapman JA, Park CK, Campos SK. A transmembrane domain and GxxxG motifs within L2 are essential for papillomavirus infection. J Virol. 2013;87(1):464-73.

47. Digiuseppe S, Keiffer TR, Bienkowska-haba M, Luszczek W, Guion LG, Müller M, Sapp M. Topography of the Human Papillomavirus Minor Capsid Protein L2 during Vesicular Trafficking of Infectious Entry. J Virol. 2015;89(20):10442-52.

48. Popa A, Zhang W, Harrison MS, Goodner K, Kazakov T, Goodwin EC, Lipovsky A, Burd CG, DiMaio D. Direct binding of retromer to human papillomavirus type 16 minor capsid protein L2 mediates endosome exit during viral infection. PLoS Pathog. 2015;11(2):e1004699.

49. Seaman MN. The retromer complex - endosomal protein recycling and beyond. J Cell Sci. 2012;125(Pt 20):4693-702.

50. Cullen PJ. Endosomal sorting and signalling: an emerging role for sorting nexins. Nat Rev Mol Cell Biol. 2008;9(7):574-82.

51. Teasdale RD, Loci D, Houghton F, Karlsson L, Gleeson PA. A large family of endosome-localized proteins related to sorting nexin 1. Biochem J. 2001;358(Pt 1):7-16.

52. Carlton J, Bujny M, Peter BJ, Oorschot VM, Rutherford A, Mellor H, Klumperman J, McMahon HT, Cullen PJ. Sorting nexin-1 mediates tubular endosome-to-TGN transport through coincidence sensing of high- curvature membranes and 3-

phosphoinositides. Curr Biol. 2004;14(20):1791-800.

53. Cullen PJ, Korswagen HC. Sorting nexins provide diversity for retromer-dependent trafficking events. Nat Cell Biol. 2012;14(1):29-37.

54. Van weering JR, Verkade P, Cullen PJ. SNX-BAR proteins in phosphoinositide-mediated, tubular-based endosomal sorting. Semin Cell Dev Biol. 2010;21(4):371-80.

55. Pylypenko O, Lundmark R, Rasmuson E, Carlsson SR, Rak A. The PX-BAR membrane-remodeling unit of sorting nexin 9. EMBO J. 2007;26(22):4788-800.

56. Collins BM, Skinner CF, Watson PJ, Seaman MN, Owen DJ. Vps29 has a phosphoesterase fold that acts as a protein interaction scaffold for retromer assembly. Nat Struct Mol Biol. 2005;12(7):594-602.

57. Rojas R, Kametaka S, Haft CR, Bonifacino JS. Interchangeable but essential functions of SNX1 and SNX2 in the association of retromer with endosomes and the trafficking of mannose 6-phosphate receptors. Mol Cell Biol. 2007;27(3):1112-24.

58. Gullapalli A, Wolfe BL, Griffin CT, Magnuson T, Trejo J. An essential role for SNX1 in lysosomal sorting of protease-activated receptor-1: evidence for retromer-, Hrs-, and Tsg101-independent functions of sorting nexins. Mol Biol Cell. 2006;17(3):1228-38.

59. Rojas R, Van vlijmen T, Mardones GA, Prabhu Y, Rojas AL, Mohammed S, Heck AJ, Raposo G, van der Sluijs P, Bonifacino JS. Regulation of retromer recruitment to endosomes by sequential action of Rab5 and Rab7. J Cell Biol. 2008;183(3):513-26.

60. Harrison MS, Hung CS, Liu TT, Christiano R, Walther TC, Burd CG. A mechanism for retromer endosomal coat complex assembly with cargo. Proc Natl Acad Sci USA. 2014;111(1):267-72.

61. Lipovsky A, Popa A, Pimienta G, Wyler M, Bhan A, Kuruvilla L, Guie MA, Poffenberger AC, Nelson CD, Atwood WJ, DiMaio D. Genome-wide siRNA screen identifies the retromer as a cellular entry factor for human papillomavirus. Proc Natl Acad Sci USA. 2013;110(18):7452-7.

62. Zhang W, Kazakov T, Popa A, Dimaio D. Vesicular trafficking of incoming human papillomavirus 16 to the Golgi apparatus and endoplasmic reticulum requires γ-secretase activity. MBio. 2014;5(5):e01777-14.

63. Aydin I, Weber S, Snijder B, et al. Large scale RNAi reveals the requirement of nuclear envelope breakdown for nuclear import of human papillomaviruses. PLoS Pathog. 2014;10(5):e1004162.

64. Day PM, Baker CC, Lowy DR, Schiller JT. Establishment of papillomavirus infection is enhanced by promyelocytic leukemia protein (PML) expression. Proc Natl Acad Sci USA. 2004;101(39):14252-7.

65. Richards RM, Lowy DR, Schiller JT, Day PM. 2006. Cleavage of the papillomavirus minor capsid protein, L2, at a furin consensus site is necessary for infection. Proc. Natl. Acad. Sci. U. S. A. 103:1522–1527.

66. Knævelsrud H, Søreng K, Raiborg C, Håberg K, Rasmuson F, Brech A, Liestøl K, Rusten TE, Stenmark H, Neufeld TP, Carlsson SR, Simonsen A. Membrane remodeling by the PX-BAR protein SNX18 promotes autophagosome formation. J Cell Biol. 2013;202(2):331-49.

67. Morris HH, Gatter KC, Sykes G, Casemore V, Mason DY. Langerhans' cells in human cervical epithelium: effects of wart virus infection and intraepithelial neoplasia. Br J Obstet Gynaecol. 1983;90(5):412-20.

68. Cunningham AL, Carbone F, Geijtenbeek TB. Langerhans cells and viral immunity. Eur J Immunol. 2008;38(9):2377–85.

69. Matthews K, Leong CM, Baxter L, et al. Depletion of Langerhans cells in human papillomavirus type 16-infected skin is associated with E6-mediated down regulation of E-cadherin. J Virol. 2003;77(15):8378-85.

70. Mota F, Rayment N, Chong S, Singer A, Chain B. The antigen-presenting environment in normal and human papillomavirus (HPV)-related premalignant cervical epithelium. Clin Exp Immunol. 1999;116(1):33-40.

71. Stanley M. HPV - immune response to infection and vaccination. Infect Agents Cancer. 2010;5:19.

72. Day PM, Thompson CD, Schowalter RM, Lowy DR, Schiller JT. Identification of a role for the trans-Golgi network in human papillomavirus 16 pseudovirus infection. J Virol. 2013;87(7):3862-70.

73. Fausch SC, Fahey LM, Da silva DM, Kast WM. Human papillomavirus can escape immune recognition through Langerhans cell phosphoinositide 3-kinase activation. J Immunol. 2005;174(11):7172-8.

74. Da silva DM, Movius CA, Raff AB, et al. Suppression of Langerhans cell activation is conserved amongst human papillomavirus α and β genotypes, but not a μ genotype. Virology. 2014;452-453:279-86.

75. Cuervo AM, Bergamini E, Brunk UT, Dröge W, Ffrench M, Terman A. Autophagy and aging: the importance of maintaining "clean" cells. Autophagy. 2005;1(3):131-40.

76. Lim JP, Wang JT, Kerr MC, Teasdale RD, Gleeson PA. A role for SNX5 in the regulation of macropinocytosis. BMC Cell Biol. 2008;9:58.